

Supporting Information

Isolated Boron Sites for Electroreduction of Dinitrogen to Ammonia

Xin Liu,^{†‡} Yan Jiao,^{*,†‡} Yao Zheng,^{†‡} Shi-Zhang Qiao^{*,†‡}

[†]School of Chemical Engineering and Advanced Materials, The University of Adelaide, Adelaide, South Australia, 5005, Australia.

[‡]Centre for Materials in Energy and Catalysis, The University of Adelaide, Adelaide, South Australia, 5005, Australia.

E-mail: * s.qiao@adelaide.edu.au; * yan.jiao@adelaide.edu.au

Supplementary Figures

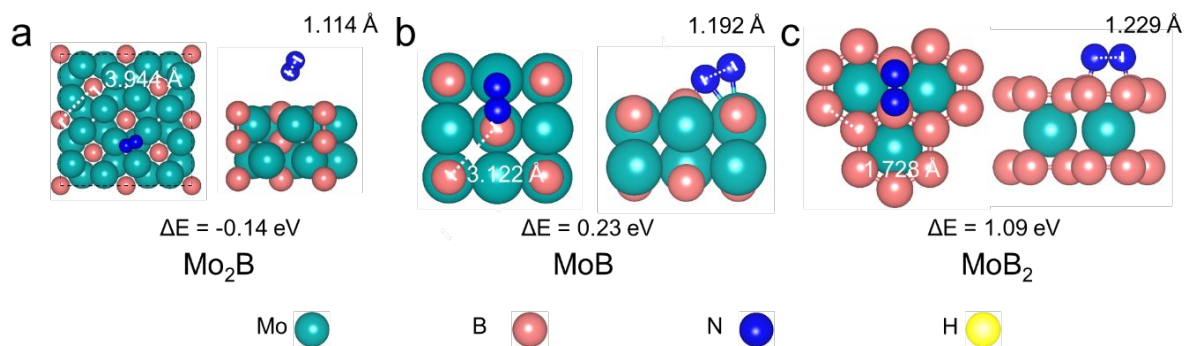


Figure S1 Atomic configurations of N_2 side-on adsorption on (a) Mo_2B , (b) $\alpha\text{-MoB}$ and (c) MoB_2 .

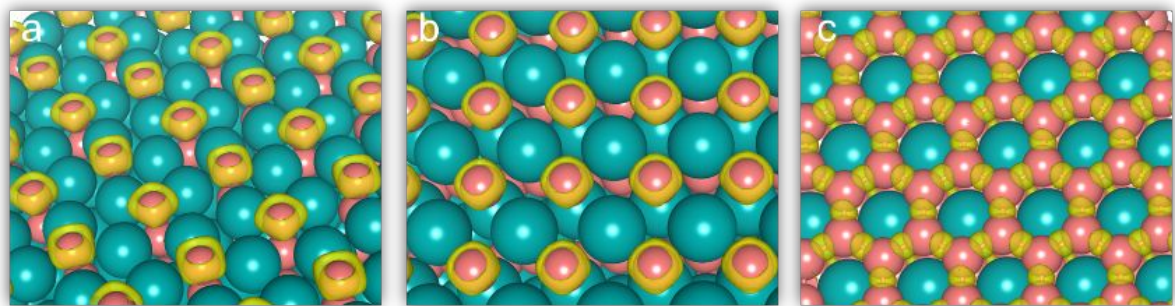


Figure S2. The electron localization function (ELF) of (a) Mo_2B , (b) $\alpha\text{-MoB}$ and (c) MoB_2 . The value of isosurface is set to 0.75 a.u.

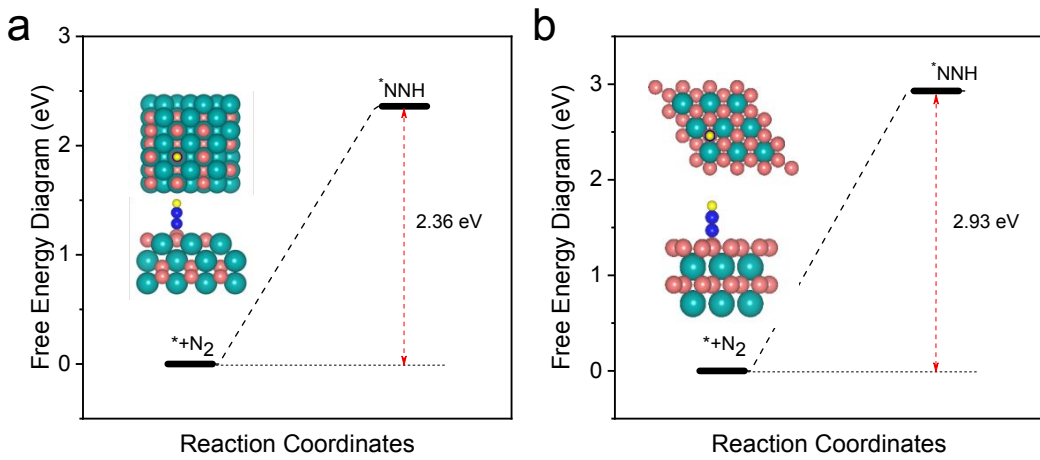


Figure S3. Free energy change of the first protonation step on (a) α -MoB and (b) MoB₂ via a distal or alternating pathway at 0V vs standard hydrogen electrode (SHE).

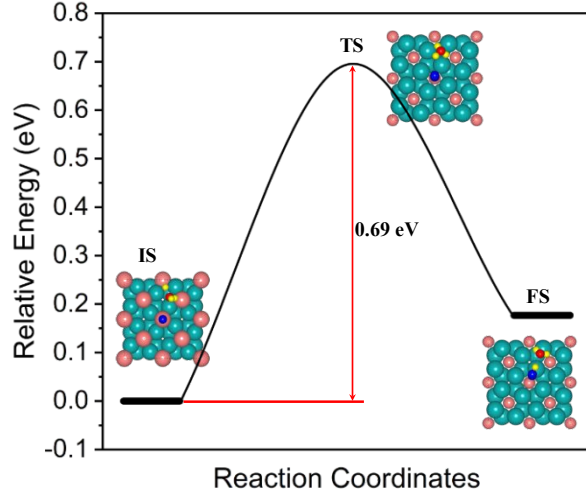


Figure S4. Kinetic barriers for the first protonation step on Mo₂B. Insets are the corresponding structures of initial (IS), transition (TS), and final states (FS). Cyan, pink, blue, red and white balls represent the Mo, B, N, O and H atoms, respectively.

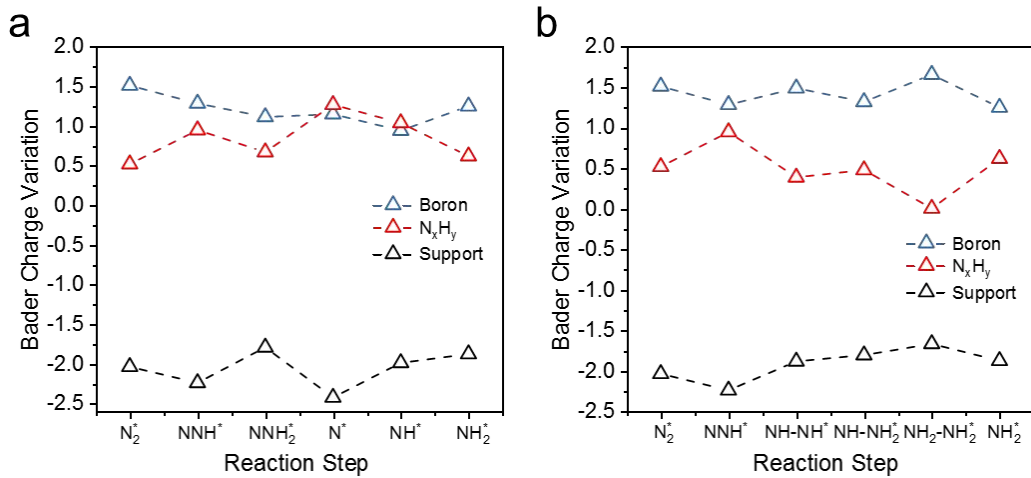


Figure S5. (a) Bader charge variation of three moieties along the (a) distal and (b) alternating pathway. Positive and negative value indicate electron accumulation and loss, respectively.

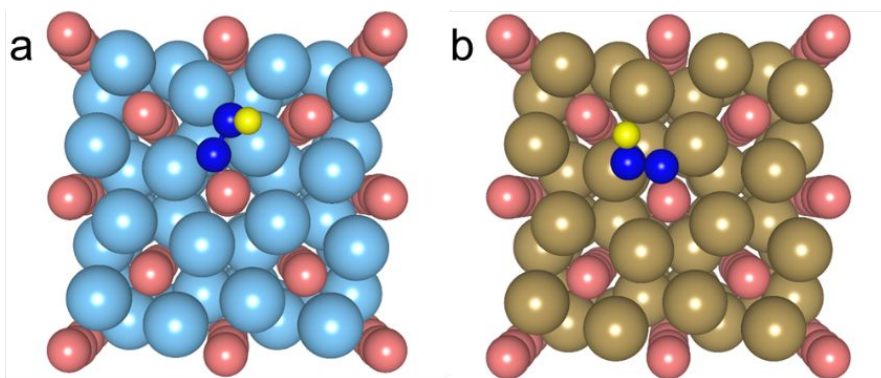


Figure S6. Atomic configuration of $*NNH$ adsorption on (a) Ti_2B and (b) Ta_2B .

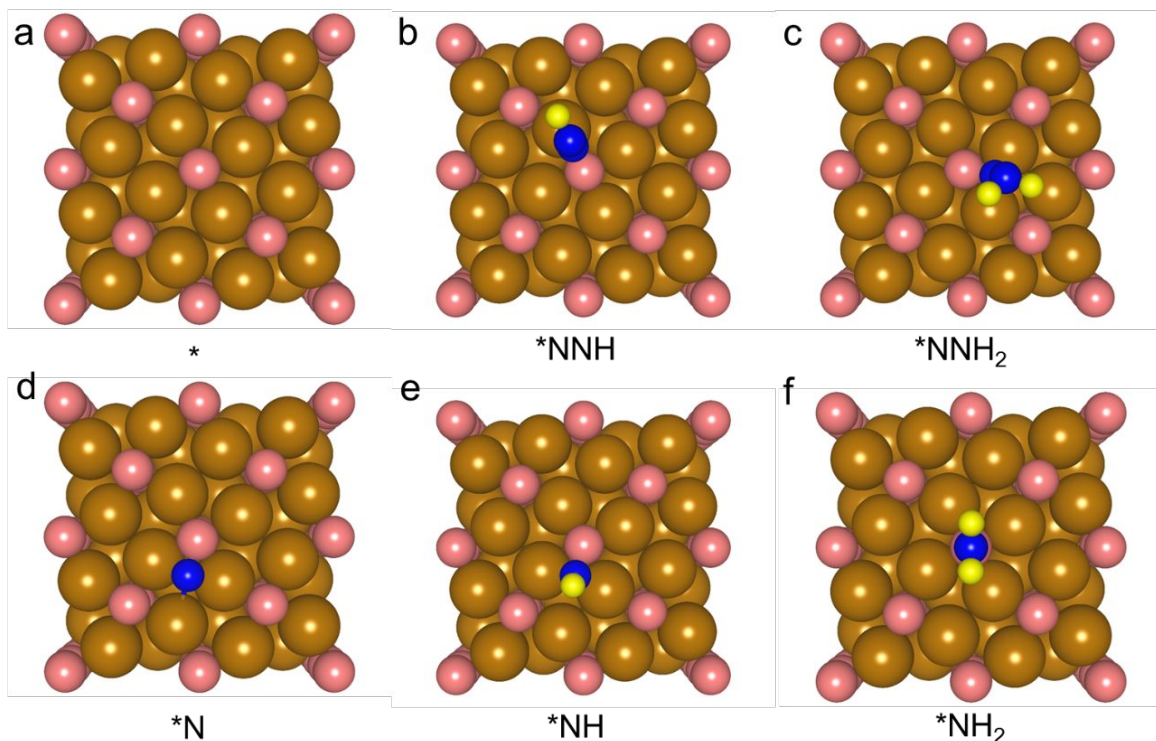


Figure S7. Atomic configurations of reaction intermediates via distal pathway of Fe_2B .

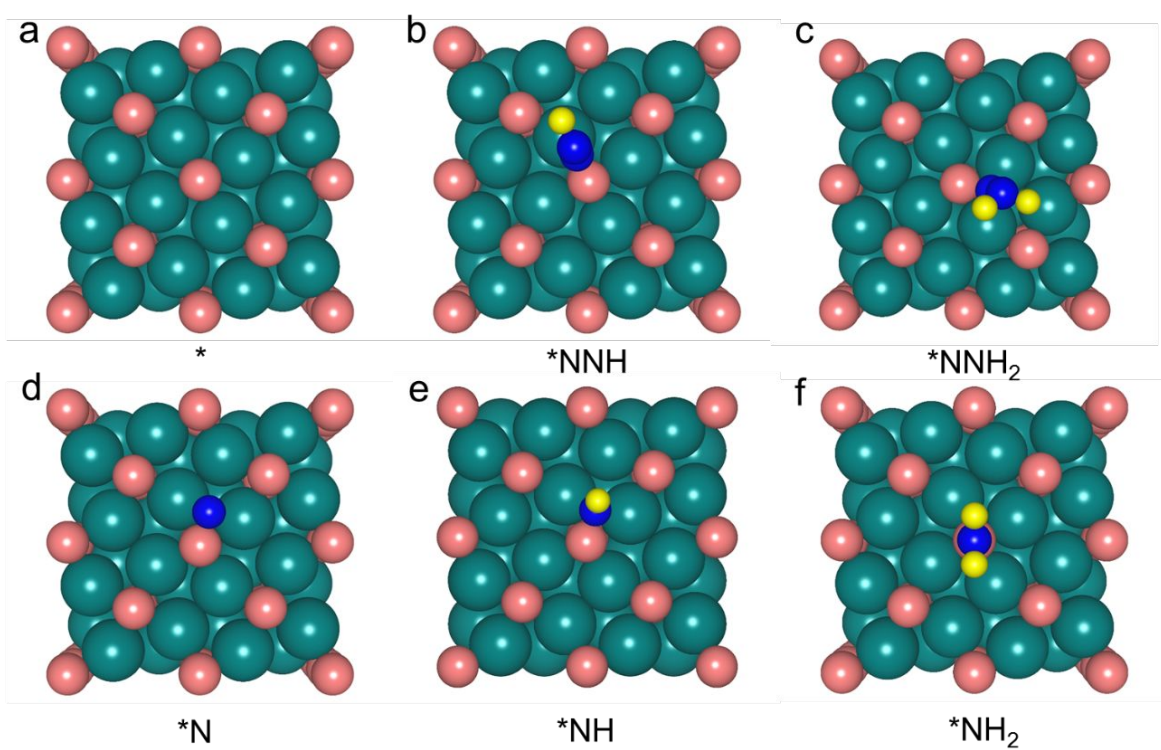


Figure S8. Atomic configurations of reaction intermediates via distal pathway of

Co_2B .

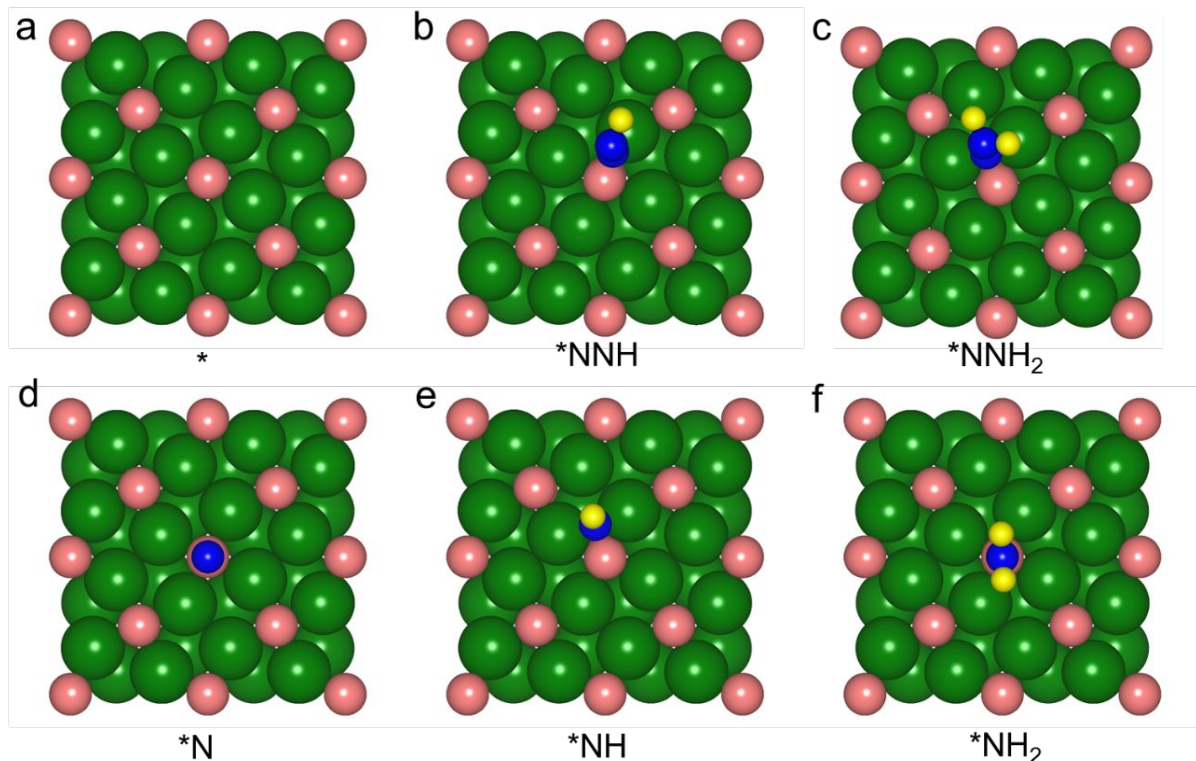


Figure S9. Atomic configurations of reaction intermediates via distal pathway of

Cr_2B .

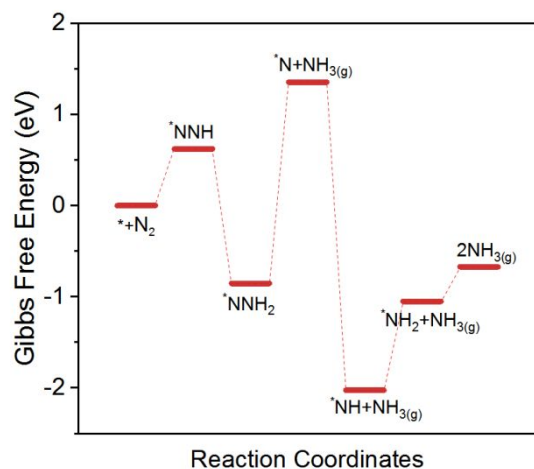


Figure S10. The free energy diagrams of eNRR via a distal pathway on Cr₂B. The third protonation step is the potential determining step with a free energy change of 2.21 eV.

Supplementary Tables

Table S1. Crystallographic information for the studied molybdenum borides.

Phase	Mo ₂ B	α-MoB	MoB ₂
Crystal system	Tetragonal	Tetragonal	Hexagonal
Space group	I4/mcm	I4 ₁ /amd	P6/mmm
a(Å)	5.56	3.13	3.03
b(Å)	5.56	3.13	3.03
c(Å)	4.78	17.05	3.35

Table S2. Crystallographic information for the studied molybdenum borides.

M ₂ B	Ti ₂ B	Cr ₂ B	Mn ₂ B	Fe ₂ B	Co ₂ B	Ni ₂ B	Ta ₂ B	W ₂ B
a(Å)	5.81	5.51	5.07	5.06	4.95	4.97	5.81	5.59
b(Å)	5.81	5.51	5.07	5.06	4.95	4.97	5.81	5.59
c(Å)	4.91	4.28	4.10	4.24	4.27	4.26	4.91	4.80

Table S3. Calculated surface energies, γ_s , for the studied metal borides.

Materials	Mo ₂ B	α-MoB	MoB ₂	Cr ₂ B	Mn ₂ B	Fe ₂ B	Co ₂ B	Ni ₂ B	W ₂ B
Surface Energy (eV/ Å)	0.202	0.180	0.155	0.285	0.346	0.277	0.219	0.138	0.168
Surface Energy (J/m ²)	3.242	2.880	2.482	4.559	5.539	4.443	3.501	2.214	2.699

Table S4. The geometric and electronic structure of molybdenum borides.

Electrocatalysts	p _x filling	p _y filling	p _z filling
Mo₂B	0.407	0.406	0.288
α-MoB	0.369	0.362	0.293
MoB₂	0.413	0.415	0.378